Preferred citation: J. Lahti, M. Dauer, D.S. Keller and U. Hirn. Linking paper structure to local distribution of deformation and damage. In **Advances in Pulp and Paper Research, Oxford 2017**, *Trans. of the XVIth Fund. Res. Symp. Oxford, 2017*, (W. Batchelor and D. Söderberg, eds), pp 669–682, FRC, Manchester, 2018. DOI: 10.15376/frc.2017.2.669.

LINKING PAPER STRUCTURE TO LOCAL DISTRIBUTION OF DEFORMATION AND DAMAGE

J. Lahti[1,2,], M. Dauer[1,2], D. S. Keller[3] and U. Hirn[1,2]*

[1] Institute of Paper, Pulp and Fiber Technology, Graz University of Technology, Inffeldgasse 23, 8010 Graz, Austria
[2] CD Laboratory for Fiber Swelling and Paper Performance, Graz University of Technology, Inffeldgasse 23, 8010 Graz, Austria
[3] Department of Chemical, Paper and Biochemical Engineering, Miami University, East High Street 650, Oh 45056 Oxford, USA

ABSTRACT

A method for quantitatively investigating the relationship between local structural properties (local basis weight, local thickness, local density and local load carrying factor (local fiber orientation)) and local tensile deformation (local strain and local temperature increase (thermal energy dissipation)) was introduced. It was found by utilizing the method for 70 g/m^2 sack paper strips that relative basis weight, relative thickness, relative density and relative load carrying factor combined explain 31% and 26% of total variation in relative strain and relative temperature increase, respectively. Best single predictors for relative strain were relative basis weight (R^2 = 0.14) and relative load carrying factor (R^2 = 0.11). On the other hand, relative basis weight alone was the best predictor for relative temperature increase (R^2 = 0.12). Finally, by analyzing the relationship between the two deformation distribution parameters from the perspective that the high relative temperature increase is preceded by the high relative strain, it could be said that the relative strain explains 45% of the total

* Corresponding author: jussi.lahti@tugraz.at

variation in the relative temperature increase (R^2 = 0.45). Thus, these two parameters describe the deformation in partially different ways. Based on this study, it can be concluded that the introduced method offers a promising tool to quantitatively investigate the separate/combined influence of local structural properties on the local deformation accumulation initializing the failure of paper.

INTRODUCTION

In-plane tensile strength of paper is of utmost importance in various coating, converting, printing and packaging applications. It is by large extend connected to a deformation distribution within paper during straining. The deformation distribution is in turn influenced by local structural non-uniformities. Previous experimental studies in this field have focused on the relationship between local basis weight and local tensile strain/damage. Wong *et al.* [1] found a correlation between local basis weight and local tensile strain, i.e. the local strain generally increased with decreasing local basis weight. Further, low basis weight regions with high local strain were found to act as a source for the rupture. Similar results were obtained by Korteoja *et al.* [2]. In addition, they found a correlation between local tensile strain and local tensile damage. The local tensile damage was studied optically with the aid of silicone impregnation which improved the visibility of the damaged regions. The strain and damage in a paper with poor formation showed a clear concentration in the low basis weight regions. Thus the strain at break of the paper decreased in relation to the local strain in the rupture zone when compared to the paper with good formation.

Yamauchi and Murakami [3] studied in turn the relationship between local basis weight and local tensile damage by utilizing infrared (IR) thermography to observe plastic deformation. This method is based on the fact that mechanical energy is converted into thermal energy in the regions where plastic deformation (damage) occurs [3]–[6]. In the case of paper with good formation, the thermal distribution was fairly uniform until the moment of rupture. The thermal distribution of papers with poor formation became in turn uneven already in an early stage of plastic deformation for most of the cases. The rupture eventually originated from one of the high temperature regions. The breaking load of the papers correlated with the thermal distribution regardless of the formation, i.e. the breaking load was higher for the papers with even thermal distribution [3].

Recently Hagman [7] also utilized IR thermography for investigating local tensile damage. In addition he measured simultaneous development of local strain and compared these two deformation distributions to local basis weight. He found

that temperature increase was high in the highly straining regions due to plastic deformation. Furthermore, he concluded that this plastic deformation took place in the regions with low basis weight.

However, the relationship between local basis weight and local tensile strain/damage is not so straightforward. The extent to which formation affects the local and global deformation of paper depends on spatial variations in various other structural factors such as fiber orientation, bonding degree, internal stresses due to drying shrinkage/wet strain, fines content and fiber density [8–9]. Variations in the structural factors lead to local stiffness variations within paper. Thus the non-uniformity of strain profile increases with the increasing (global) strain of the paper – especially beyond elastic deformation of the paper [2], [8], [10]–[12]. Damage in the highly strained regions through breakage of interfiber bonds causes redistribution of stresses to the unbroken regions, and thus increases the strain heterogeneity in the paper. With further straining one of the damaged regions grows to a macroscopic crack which causes total failure by propagating through the paper [9], 13].

The aim of this study is to advance the understanding of local distribution of deformation and damage from the current – mostly qualitative – description to a more quantitative analysis of the structural reasons for paper failure. To achieve this aim a method enabling a systematic and quantitative linking of local structural properties (basis weight, thickness, density and fiber orientation) to deformation distributions (strain and energy dissipation) is presented and utilized.

MATERIALS AND METHODS

In this study the local structural properties of four 70 g/m^2 sack paper strips are linked to their deformation distributions just prior to tensile rupture as shown in Figure 1. Local basis weight, thickness, density and fiber orientation (FO)

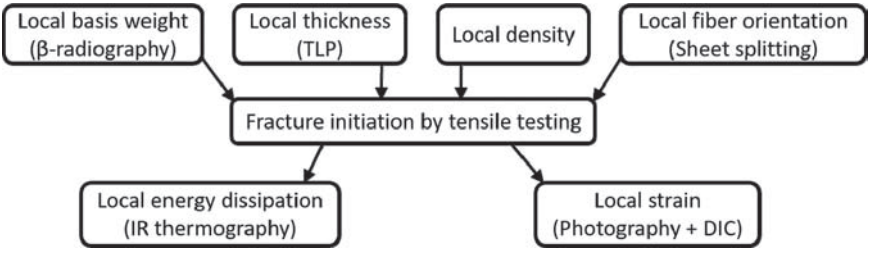

Figure 1. Principle for linking local structural properties of paper to its deformation distribution just prior to tensile rupture.

were the structural properties determined. Deformation distributions were in turn investigated by measurement of local strain and temperature increase (thermal energy dissipation) simultaneously during tensile testing.

Deformation distribution (Tensile tester, IR thermography & Photography + DIC)

The set-up for measurement of deformation distributions is shown in Figure 2. The local strain was determined on the front side of the tensile tester (Zwick/Roell Z010) with a digital single-lens reflex (SLR) camera (Nikon D5100) combined with a macrolens (Nikon ED AF Micro Nikkor 200 mm 1:4 D) and subsequent digital image correlation (DIC) analysis [14]. The frame rate and resolution of the recording were 30 Hz and 37 μm/pixel, respectively. DIC analysis was conducted with a subset size of 20 × 20 pixels and thus the strain map resolution became 0.74 mm/pixel. The determined strain map was then resized (MATLAB imresize function) to the size just prior to rupture based on the global strain of the paper strip. In order to enable an accurate DIC analysis, random speckle pattern was printed (HP Color LaserJet 4700n) on the paper before testing. The local temperature increase (thermal energy dissipation) was in turn recorded on the back side with an infrared (IR) camera (Optris PI 450). More precisely, it was determined by resizing the IR image of the paper strip before straining to the same size as the IR image just prior to rupture (MATLAB imresize function) and then subtracting the unstrained IR image from the strained one. The frame rate and resolution of the recording were 80 Hz and 0.38 mm/pixel.

The tensile test was performed under a standard climate of 23 °C and 50% relative humidity by straining the paper strips with dimensions of 40 × 65 mm^2 in machine direction (MD) with a rate of 40 mm/min. Simultaneously the local strain

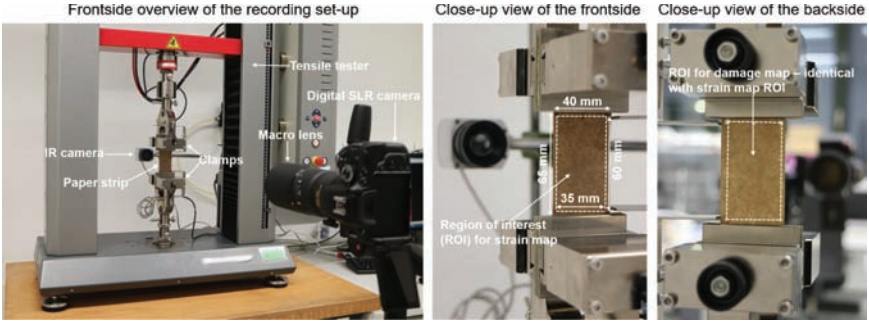

Figure 2. Set-up for recording both local strain (photography + DIC) and local temperature increase (IR thermography) simultaneously during tensile testing.

and temperature increase were recorded within the region of interest (ROI) of 35×60 mm^2 (approx. 35×61 mm^2 just prior to rupture). The ROI was marked identically on the both sides of the paper strips with four landmark dots before testing. The frontside marking was done with a felt pen whereas silver ink was needed on the backside. This was due to the high UV reflectance of silver which makes the landmark dots clearly visible in the recorded images. The tensile test was not performed until complete rupture of the strip but stopped just prior to/during rupture, i.e. at the strain level of 0.022. The reason was because the measurement of local fiber orientation is also a destructive method, and thus the local structural properties were measured after the measurement of deformation distributions.

Local basis weight (β-radiography)

The local basis weight was measured with a β-radiographic transmission method described in detail by Keller and Pawlak [15]. First the β-radiographic transmission through the paper strip and references with known basis weights was recorded on storage phosphor screen in a Formex Betaformation Box (Science Imaging Scandinavia AB). Second the screen was scanned (Fujifilm BAS 1800-II) and the local basis weights of the strip were calculated with a resolution of 50 μm/pixel by using the references. The silver landmark dots were also clearly visible in the basis weight maps.

Local thickness (TLP)

The local thickness was measured with a twin laser profilometer (TLP) described in detail by Keller *et al.* [16]. TLP determined the surface topography of the paper strip simultaneously on both sides with the aid of two lasers. The local thickness was then calculated with a resolution of 100 μm/pixel by using the surface topographies. The silver landmark dots were also clearly visible in the thickness maps.

Local fiber orientation (Sheet splitting)

The local FO was measured with a sheet splitting method described in detail by Hirn and Bauer [17]. First the paper strip was split in thickness direction (ZD) into thin layers. The number of layers was 13–18 per paper strip. The layers were subsequently scanned with a resolution of 13 μm/pixel. The landmark dots were made visible in the layers by hole punching. Second each scanned layer was analyzed through image analysis. In other words, each scanned layer was divided into subsets of 1×1 mm^2 followed by a determination of fiber orientation distribution within each subset. The fiber orientation map for all the layers in local 1×1 mm^2 subsets was then determined by averaging the fiber orientation distributions of the layers in ZD and

subsequently fitting orientation ellipses to the averaged distributions. For linking the local fiber orientation to the local ability to carry tensile load, a variable called load carrying factor was introduced. It is defined as the portion of fibers pointing in MD and it is calculated by using the polar equation of an (orientation) ellipse as follows:

$$2r = \frac{2ab}{\sqrt{(b\cos\theta)^2 + (a\sin\theta)^2}} \quad (1)$$

where *2r* is the load carrying factor (MD portion of the fibers), *a* is the major semi-axis of the ellipse, *b* is the minor semi-axis of the ellipse and Θ is the FO angle (*deg.*).

Registration and correlation analysis

In order to enable a quantitative pointwise correlation, the measured maps were aligned with a resolution of 1 mm/pixel. This was done through landmark based registration by utilizing the four landmark dots visible in the corners of each map. Subsequently the registered maps were aligned with a shape preserving coordinate transform. This procedure is described in detail by Hirn and Bauer [18]. At this point the density map was also calculated by dividing the aligned basis weight map with the aligned thickness map. The noise of the aligned maps was then reduced by the aid of Gaussian low pass filter with a kernel size of 5 × 5 and standard deviation of 1.0. For the quantitative pointwise correlation local relative values were calculated for each property, i.e. the average of the property map was subtracted from the local property value. Finally the quantitative pointwise relationship between deformation distribution maps and structural maps was conducted by correlation coefficient (*r*), simple/multiple linear regression and analysis of variance (ANOVA) [19].

RESULTS AND DISCUSSION

Figure 3 shows the determined relative basis weight, relative thickness, relative density, relative load carrying factor, relative strain and relative temperature increase maps for one of the studied paper strips. The maps were made a little bit smaller than the ROI in order to remove the effect of the landmark dots from the statistical analysis. By observing the maps similar conclusions can be made as in the previous investigations described in the introduction section of this paper. In other words, both the local relative strain and relative temperature increase seem to correlate to a certain extent with the local relative basis weight. Similarities can be also seen between the two deformation distribution maps. Furthermore, the other structural maps seem to correlate to a certain extent with the two deformation

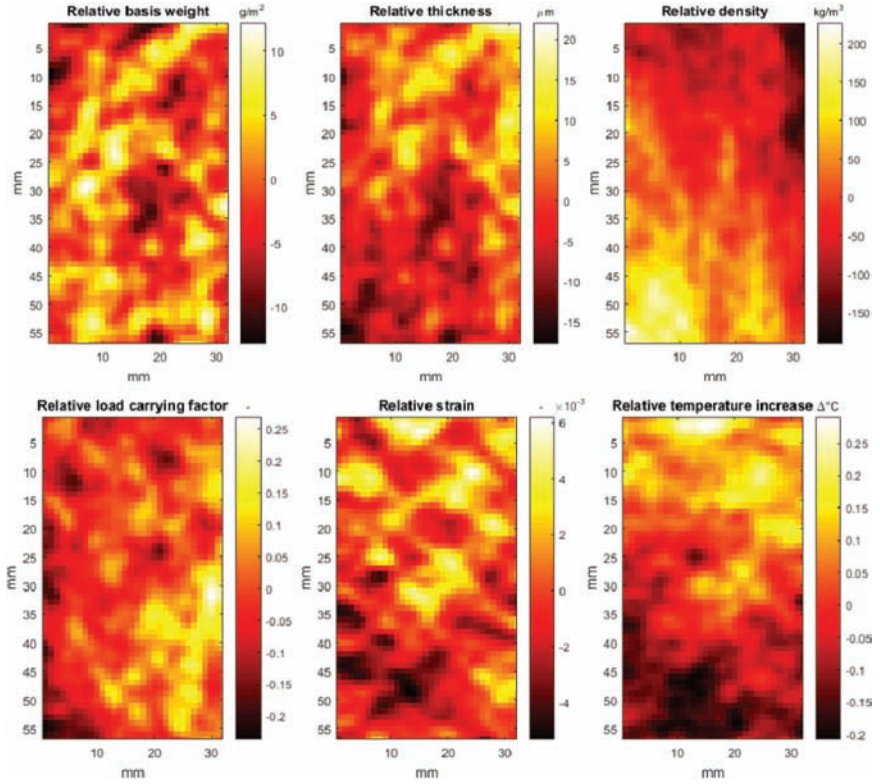

Figure 3. Relative basis weight, relative thickness, relative density, relative load carrying factor, relative strain and relative temperature increase maps for one of the studied paper strips.

distribution maps as well. In order investigate these causalities in a more detailed and systematic manner a quantitative statistical analysis is utilized next.

The quantitative statistical analysis is started by studying the pointwise (pixel-wise) correlations between relative strain maps and relative structural maps of the four paper strips. Figure 4 shows scatterplots describing these relationships. It can be seen that a moderate negative linear correlation exists between relative strain and relative basis weight ($r = –0.38$). Furthermore, by fitting linear regression model and calculating coefficient of determination (R^2), it can be said that the relative basis weight explains 14% of the total variation in relative strain ($R^2 = 0.14$). No correlation is in turn present between relative strain and relative thickness ($r = –0.01$ and $R^2 = 0.00$). Interestingly, a moderate negative linear correlation exists also between

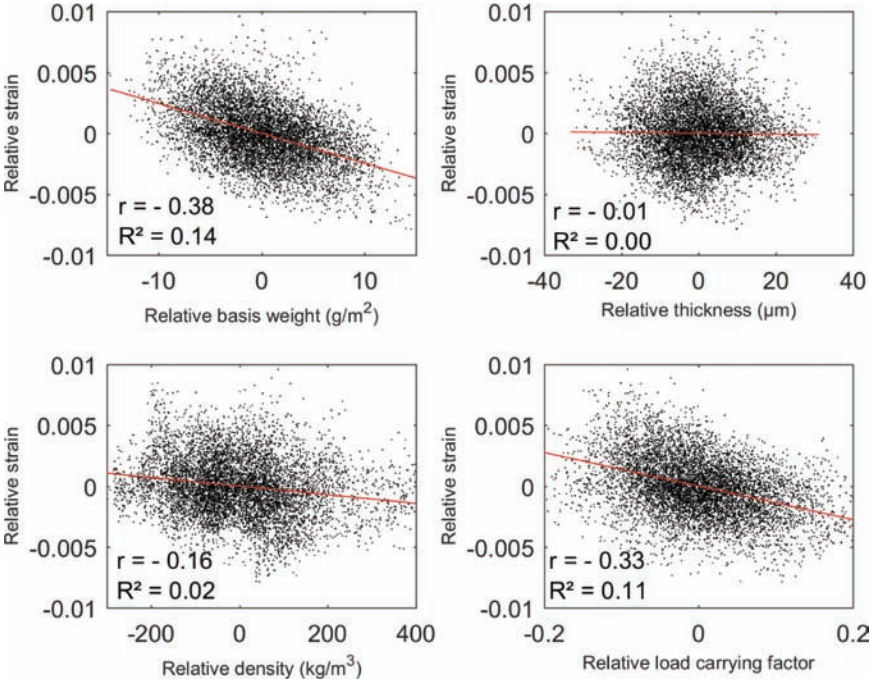

Figure 4. Scatterplots showing the pointwise (pixelwise) relationships between relative strain maps and relative structural maps (all four paper strips included). Quantitative statistical analysis conducted by fitting simple linear regression model (line), calculating linear correlation (r) and conducting ANOVA (R^2).

relative strain and relative load carrying factor ($r = –0.33$). The relative load carrying factor is capable of explaining 11% of the total variation in relative strain ($R^2 = 0.11$), i.e. it is only a slightly weaker predictor for relative strain than relative basis weight. Finally, a weak negative linear correlation is present between relative strain and relative density ($r = –0.16$). The relative density explains 2% of total variation in relative strain ($R^2 = 0.02$).

In Figure 5 scatterplots describing the pointwise relationships between relative temperature increase maps and relative structural maps of the four paper strips are shown. It can be seen that the strength of the negative linear correlation between relative temperature increase and relative basis weight ($r = –0.35$) is at the same level with the correlation between relative strain and relative basis weight. The relative basis weight explains 12% of the total variation in relative temperature increase ($R^2 = 0.12$). However, only a weak negative linear correlation is present

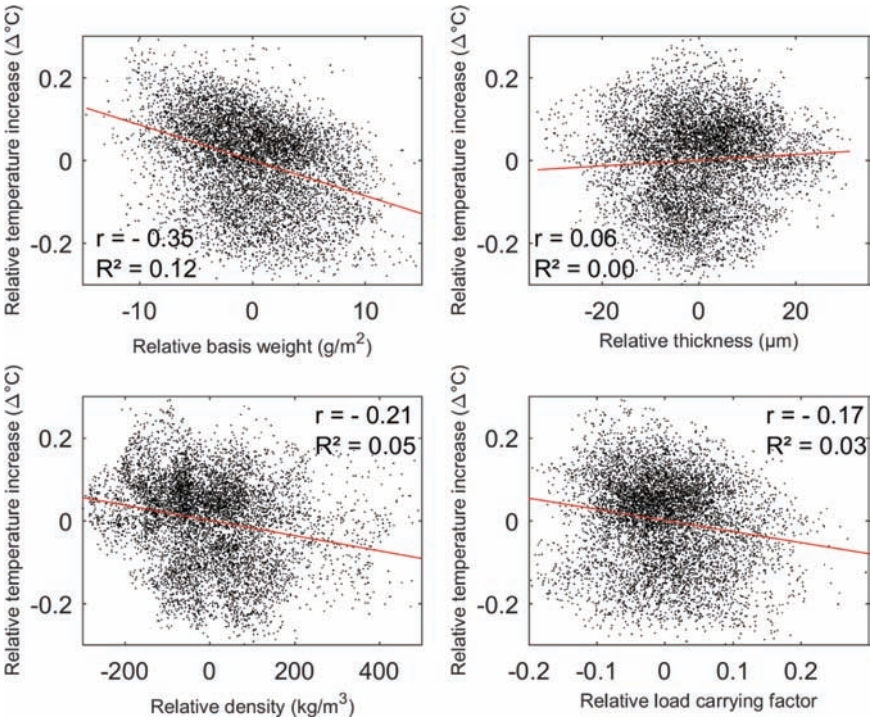

Figure 5. Scatterplots showing the pointwise (pixelwise) relationships between relative temperature increase maps and relative structural maps (all four paper strips included). Quantitative statistical analysis conducted by fitting simple linear regression model (line), calculating linear correlation (r) and conducting ANOVA (R^2).

between relative temperature increase and relative load carrying ability ($r = –0.17$). The relative load carrying ability is capable of explaining only 3% of the total variation in relative temperature increase ($R^2 = 0.03$). On the other hand, the linear negative correlation is stronger between relative temperature increase and relative density ($r = –0.21$) in comparison to the correlation between relative strain and relative density. The relative density explains 5% of the total variation in relative temperature increase ($R^2 = 0.05$). As in the case of relative strain and relative thickness, no correlation exists between relative temperature increase and relative thickness ($r = 0.06$ and $R^2 = 0.00$).

So far simple linear regression model has been utilized to study the relationships between deformation distribution maps and structural maps. In the following the analysis is extended to multiple linear regression model. This means that the

relative strain and temperature increase are modelled as a linear function of relative basis weight, relative thickness, relative density and relative load carrying factor. Figure 6 shows a scatterplot describing the pointwise relationship between modelled relative strain maps and measured relative strain maps of the four paper strips. The analysis revealed that the structural properties combined explain 31% of the total variation in relative strain ($R^2 = 0.31$). In other words, the relative basis weight, relative thickness, relative density and relative load carrying factor are locally able to predict the relative strain to a degree of 31%.

In Figure 7, a scatterplot describing the pointwise relationship between modelled relative temperature increase maps and measured relative temperature increase maps of the four papers is shown. Based on the analysis it can be said that the structural properties combined are capable of predicting the relative temperature increase to a degree of 26%. This means that the structural properties predict the local relative strain only slightly better than the local relative temperature increase. The remaining differences of R^2 to 1 are 0.69 and 0.74 for the relative strain/structural properties and the relative temperature increase/structural properties, respectively. These differences can be explained with other influence factors, i.e. paper strip geometry, other structural variables not measured, inaccuracies/noise in the

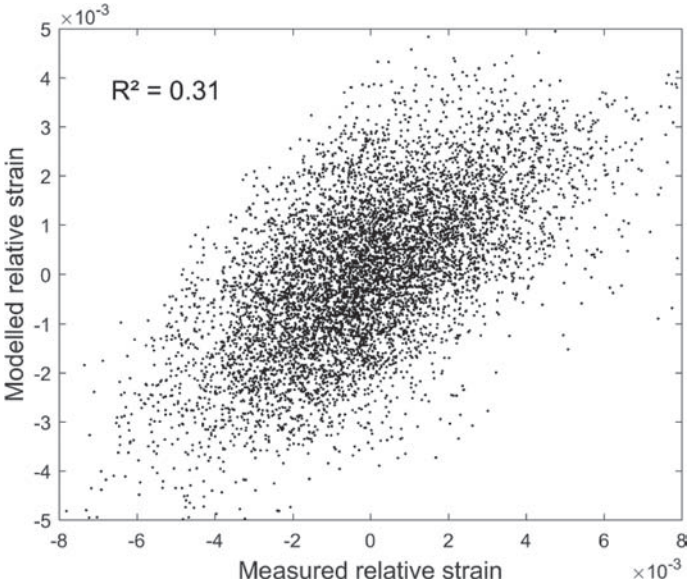

Figure 6. Scatterplot showing the pointwise relationship between modelled relative strain maps and measured relative strain maps (all four paper strips included). Quantitative analysis conducted by fitting multiple linear regression model and conducting ANOVA (R^2).

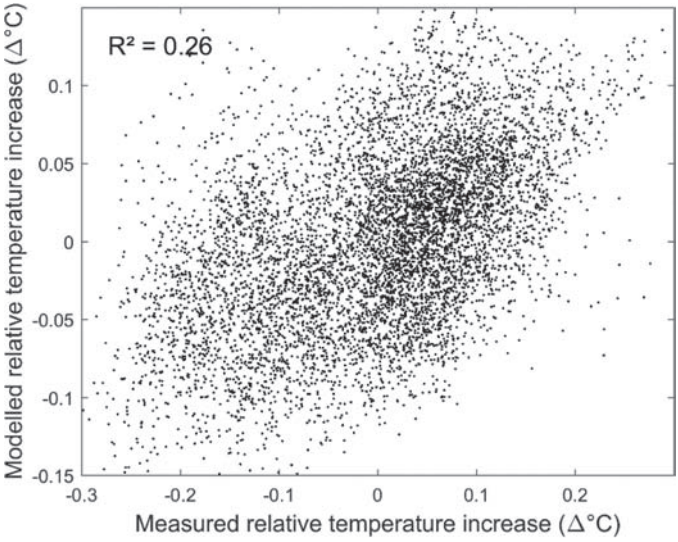

Figure 7. Scatterplot showing the pointwise relationship between modelled relative temperature increase maps and measured relative temperature increase maps (all four paper strips included). Quantitative analysis conducted by fitting multiple linear regression model and conducting ANOVA (R^2).

measurements, registration errors, etc. Especially by increasing the length to width ratio of the investigated paper strips, the effect of lateral constraint caused by the clamps of the tensile tester could be reduced. In other words, the relationship between local structural properties and local tensile deformation might become stronger by taking the physics of the tensile test better into account.

Finally the two different methods for measuring deformation distribution are compared. Figure 8 shows a scatterplot describing the pointwise (pixelwise) relationship between relative temperature increase maps and relative strain maps of the four paper strips. It can be seen that a positive linear correlation exists between these two damage distributions ($r = 0.67$). In the introduction section of this paper it was described that locally varying structural factors lead to an uneven strain distribution within paper strip. Subsequently, damage occurs in the highly strained regions through breakage of interfiber bonds – observable by local thermal energy dissipation (local temperature increase). By analyzing the relationship between relative strain and relative temperature increase from this perspective, it could be said that the relative strain explains 45% of the total variation in the relative temperature increase ($R^2 = 0.45$). This means that the remaining difference to 100% is 55% and other influence factors play a strong role. It is highly unlikely that all of this

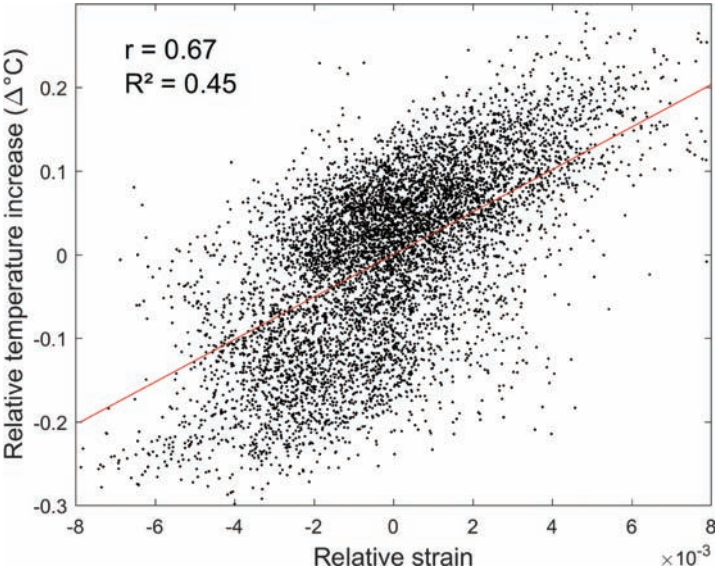

Figure 8. Scatterplot showing the pointwise (pixelwise) relationship between relative strain maps and relative temperature increase maps (all four paper strips included). Quantitative statistical analysis conducted by fitting simple linear regression model (line), calculating linear correlation (r) and conducting ANOVA (R^2).

remaining difference can be explained with the measurement/analysis related inaccuracies, and thus it can be said that the relative strain and the relative temperature increase describe the deformation in partially different ways.

CONCLUSIONS

Combining measurement of local structural properties, measurement of local tensile deformation and registration of the measured local values provides a promising method to quantitatively investigate the separate/combined influence of different structural parameters on the localized deformation initializing the failure of paper.

It was found by utilizing the method for sack paper strips that relative basis weight, relative thickness, relative density and relative load carrying factor combined explain 31% and 26% of the total variation in relative strain and relative temperature increase, respectively. Best single predictors for relative strain were relative basis weight ($R^2 = 0.14$) and relative load carrying factor ($R^2 = 0.11$). On the other

hand, relative basis weight alone was the best predictor for relative temperature increase ($R^2 = 0.12$). Finally, by analyzing the relationship between the two deformation distribution parameters from the perspective that high relative temperature increase is preceded by high relative strain, it could be said that the relative strain explains 45% of the total variation in the relative temperature increase ($R^2 = 0.45$). Thus, these two parameters describe the deformation in partially different ways.

ACKNOWLEDGEMENTS

The authors greatly appreciate Mondi, Océ, the Austrian Federal Ministry of Economy, Family and Youth and the Austrian National Foundation for Research, Technology and Development for the financial support.

REFERENCES

1. L. Wong, M. T. Kortschot and C. T. J. Dodson (1996), Effect of formation on local strain fields and fracture of paper, *JPPS*, **22**(6): 213–219.
2. M. J. Korteoja, K. J. Niskanen, M. T. Kortschot and K. K. Kaski (1998), Progressive damage in paper, *Pap Puu*, **80**(5): 364–372.
3. T. Yamauchi and K. Murakami (1994), Observation of deforming process of a poorly formed papersheet by thermography, *Sen'i Gakkaishi*, **50**(9): 424–425.
4. D. P. Dumpleton, K. P. Kringstad and C. Söremark (1973), Temperature profiles in paper during straining, *Svensk Papperstid*, **14**: 521–528.
5. C. Hyll, H. Vomhoff and M. Nygårds (2012), Analysis of the plastic and elastic energy during the deformation and rupture of a paper sample using thermography, *NPPRJ*, **27**(2): 329–334.
6. T. Yamauchi (2012), 'Application of IR thermography for studying deformation and fracture of paper,' Ch. 1 in R. Prakash (ed.), *Infrared Thermography*, InTech.
7. A. Hagman (2016), Influence of inhomogeneities on the tensile and compressive mechanical properties of paperboard, Doctoral Thesis, Department of Solid Mechanics, KTH, Stockholm.
8. M. J. Korteoja, A. Lukkarinen, K. Kaski, D. E. Gunderson, J. L. Dahlke and K. J. Niskanen (1996), Local strain fields in paper, *Tappi J*, **79**(4): 217–224.
9. M. Alava and K. Niskanen (2008), 'In-plane tensile properties,' Ch. 5 in K. Niskanen (ed.), *Paper Physics Paperi ja Puu*.
10. R. J. Norman (1966), 'Dependence of sheet properties on formation and forming variables,' in *Consolidation of the Paper Web*, *Trans. 3rd Fund. Res. Symp.*, (F. Bolam (ed.)), pp. 269–298, BPBMA, London.
11. M. J. Korteoja, A. Lukkarinen, K. Kaski and K. J. Niskanen (1997), Computational study of formation effects on paper strength, *JPPS*, **23**(1): 18–22.

12. A. Hagman and M. Nygårds (2012), Investigation of sample-size effects on in-plane tensile testing of paperboard, *NPPRJ*, **27**(2): 295–304.
13. J. M. Considine, C. T. Scott, R. Gleisner and J. Y. Zhu (2006), 'Use of digital image correlation to study the local deformation field of paper and paperboard,' in *Advances in Paper Science and Technology*, *Trans. 13th Fund. Res. Symp.*, pp. 613–630, BPBMA, London.
14. C. Eberl, R. Thompson, D. Gianola, W. Sharpe Jr and K. Hemker (2006), Digital image correlation and tracking. MatLabCentral, Mathworks file exchange server, FileID 12413.
15. D. S. Keller and J. J. Pawlak (2001), β-radiographic imaging of paper formation using storage phosphor screens, *JPPS*, **27**(4): 117–123.
16. D. S. Keller, D. L. Branca and O. Kwon (2012), Characterization of nonwoven structures by spatial partitioning of local thickness and mass density, *J Mater Sci*, **47**(1): 208–226.
17. U. Hirn and W. Bauer (2007), 'Evaluating an improved method to determine layered fiber orientation by sheet splitting,' in Proc. *61st annual APPITA Conference & 2007 Paper Physics Conference*, pp. 71–80.
18. U. Hirn, M. Lechthaler and W. Bauer (2008), Registration and point wise correlation of local paper properties, *NPPRJ*, **23**(4): 374–381.
19. J. Neter, M. Kutner, C. Nachtsheim and W. Wassermann (1996), *Applied Linear Statistical Models*, McGraw-Hill.

Transcription of Discussion

LINKING PAPER STRUCTURE TO LOCAL DISTRIBUTION OF DEFORMATION AND DAMAGE

J. Lahti,[1,2] *M. Dauer,*[1,2] *D. S. Keller*[3] *and U. Hirn*[1,2]

[1] Institute of Paper, Pulp and Fibre Technology, Graz University of Technology, Inffeldgasse 23, 8010 Graz, Austria
[2] CD Laboratory for Fibre Swelling and Paper Performance, Graz University of Technology, Inffeldgasse 23, 8010 Graz, Austria
[3] Department of Chemical, Paper and Biochemical Engineering, Miami University, East High Street 650, OH 45056 Oxford, OH, USA

Kit Dodson University of Manchester

It is very appealing work and as a theoretician it's the kind of gift that we like to have. You have so much detailed data and the local correlations are extremely exciting. I think the biggest new contribution is the relationships to damage. However, if we could look at the slide which shows the strain against the local grammage, I have made some contribution in that area. Some years back, I calculated analytically a slope of that regression line. I will send you a reference to it.

Georg Goetz SIG Combibloc

Very interesting work. When you looked at the correlations, you always looked at the correlations between two variables. Did you also analyze multivariable correlations to see if there are higher order correlations between some of the parameters?

Discussion

Jussi Lahti Graz University of Technology

I didn't present it here, but I also calculated the combined influence of all the structural properties. This significantly increases the correlation when you put them all together.

Anton Hagman RISE BioEconomy

I have two questions; the first one is just to check your method, you strained the sample while photographing it with the thermal camera and the video camera, and then you took it out and made the radiography and thickness measurements. Did you keep it strained while you did this, because otherwise it should shrink back a bit, and I think maybe that would cause some noise in the correlations?

Jussi Lahti

No. I didn't. In general, the strain map has to be scaled to the same size as the other maps measured after unloading. So there might be a small error in this respect, but it should not be significant in this kind of paper where the strain, ~2%, is quite low. However, if you study highly extensible papers then there might be more inaccuracy.

Anton Hagman

And then my second question, I saw some interesting graphs here in your presentation that are not in the Proceedings, such as the ones with the temperature versus strain. Will they show up in some other place?

Jussi Lahti

The thing was that I only recently got them ready and I wanted to present them here, so unfortunately I was not able to include them in the proceedings, but they be published later.

Bill Sampson University of Manchester

I think you were right to be looking at the neighbouring properties of individual pixels, and I think that it will be very interesting to bring some multidimensional analysis to that. But my question concerns the scales at which you are looking. These are pixel-size observations, correct? And your pixel size is quite small, I think.

Jussi Lahti

It is 1 square millimetre.

Bill Sampson

Okay, and you say it is a sack paper, so we would expect some quite large fibres. You have different scales of interest in this structure: you have the fibre length, you have some characteristic cluster size, etc., and I think it would be worth doing analysis from your beta radiographs, there are many available in the literature, to identify some key scales that are of interest for this debate.

Petri Mäkelä BillerudKorsnas AB

The graphs in Figure 4 of your article show data points for the complete test piece area. However, in your presentation introduction, you started that your aim was to understand failure initiation under tensile loading. Failure initiation in paper materials subjected to tension is a local phenomenon, where the failure generally is initiated at a weak spot region of the material. Consequently, only few of the data points that you present in Figure 4 are associated with the failure initiation process. You should be able to figure out a region of interest for the failure initiation process based on your IR thermography measurements. Have you checked where the subset of data points corresponding to failure initiation region are located in the graphs of Figure 4?

Jussi Lahti

Yes, first of course more in a qualitative manner, to think about how to analyse the data. I was checking the property maps and then we looked at the points where we saw the strongest strain and damage, and then we looked at the points where nothing happens. This is how we reduced points and focused more to the extreme regions.

Petri Mäkelä

Okay. Yes, I understand that the points you are talking about now are the points that you found in your IR.

Jussi Lahti

Yes, this is now an example of the highly straining regions on top of the basis weight map, but I did this kind of analysis for strain versus all the structural

properties and temperature increases versus all the structural properties, so this is just an example then of the correlations that are shown in this graph.

Ron Peerlings Eindhoven University of Technology

As a follow up on this question, what you could try to do is compute correlations between damage and all high strains and that should show you patterns if there are any patterns in these samples that you have measured.

Jussi Lahti

Yes, I had been thinking quite a lot about how to efficiently analyze these things.